

Influence of the Nd³⁺ Moments on the Magnetic Behaviour of the Oxypnictides superconductors NdFeAsO_{1-x}F_x

Jan-Willem G. Bos¹, Peter Jeglič², Emmanuelle Suard³, Michela Brunelli⁴, Denis Arčon^{2,5*} and Serena Margadonna^{1*}

¹School of Chemistry, University of Edinburgh, West Mains Road, EH9 3JJ Edinburgh, UK.

²Institute "Jozef Stefan", Jamova 39, 1000 Ljubljana, Slovenia.

³Institute Laue-Langevin, Grenoble, France.

⁴European Synchrotron Radiation Facility, BP 220, 38043 Grenoble Cedex, France.

⁵Faculty of Mathematics and Physics, University of Ljubljana, Jadranska 19, 1000 Ljubljana, Slovenia.
email: serena.margadonna@ed.ac.uk and denis.arcon@ijs.si

The rare-earth oxypnictides with general formula REFeAsO (RE = La, Ce, Pr, Nd, Sm, Gd, Tb, Dy) are currently attracting much interest due to the observation of superconductivity upon chemical doping with critical temperatures only surpassed by the high-T_c cuprates. It is now established that in electron doped LaFeAsO superconductivity appears in the close vicinity of a spin density wave (SDW) instability implying that magnetic correlations play an important role in determining the ground state properties. In order to elucidate the influence of magnetic interactions on the unconventional superconducting properties, it is fundamental to study the behaviour of related materials containing different RE ions with unpaired *4f* electrons such as Nd³⁺. Here we report on our studies of the properties of NdFeAs(O_{1-x}F_x) (*x* = 0, 0.15) which display a much more complex magnetic phase diagram than the La based family of superconductors. Neutron and X-ray powder diffraction, magnetic susceptibility, resistivity measurement and ⁷⁵As nuclear magnetic resonance (NMR) were employed to investigate their structural and magnetic response. Long range magnetic ordering of the Fe²⁺ sublattice was not observed in the parent compound NdOFeAs down to 1.6 K. Instead, three-dimensional antiferromagnetic ordering of the Nd³⁺ ions develops at very low temperatures (below 5 K). The ⁷⁵As nuclear magnetic resonance (NMR) shows that the magnetic ground state of the parent compound NdFeAsO is highly disordered below ~ 140 K with large spatial spin or charge inhomogeneities. The F⁻ doped (*x* = 0.15) material with a superconducting transition temperature *T*_C = 43(1) K shows a strongly temperature dependent ⁷⁵As NMR shift and spin-lattice relaxation rate. Both parameters increase with decreasing temperature in striking contrast to the behavior observed for the La-based samples. Our results show that the RE ions are not innocent spectators and that their magnetic moment introduce extra degrees of freedom into the system strongly influencing the ground state properties.

Introduction:

The family of rare-earth quaternary oxypnictides with general formula REFeAsO (RE = La, Sm, Ce, Nd, Pr, Gd, Tb, Dy)¹ is currently generating much excitement in the condensed matter community. When electron or hole doped, these materials are reported to display superconductivity with superconducting transition temperatures, T_C , as high as 55 K, being surpassed only by the high- T_C cuprates.²⁻¹¹ In analogy with the cuprates, the quaternary oxypnictides adopt a layered structure (space group $P4/nmm$ – featuring alternating tetrahedrally coordinated RE-O and Fe-As layers along the c -axis) in which the role of the conducting copper-oxygen plane is played by the Fe-As layer. Superconductivity in the high- T_C cuprates occurs upon doping the parent compound La_2CuO_4 , which is a Mott-Hubbard insulator and displays strong 2D antiferromagnetic interactions. Similarly, doping of the parent compounds REFeAsO (e.g. partial replacement of the O^{2-} with F^- , oxygen deficiency or substitution of the RE with Sr^{2+} in the insulating RE-O layer) provides extra charge in the conduction plane triggering the occurrence superconductivity. However, unlike La_2CuO_4 , the REFeAsO parent materials are not insulators but bad metals or semimetals and a strong covalency in the FeAs plane has been suggested.¹²

It has now been shown that in electron doped LaFeAsO superconductivity appears in the close vicinity of a spin density wave (SDW) ground state implying that magnetic correlations may be important in the promotion of the superconducting ground state. La^{3+} has no unpaired electrons and the magnetic response can be attributed only to the $\text{Fe}^{2+} 3d^6$ electronic states that dominate the region around the Fermi level. Resistivity and magnetic susceptibility measurements show that at high temperatures LaFeAsO has a Pauli-like spin susceptibility while on cooling anomalies are observed at 156 and 138 K, which are linked to a structural phase transition (tetragonal (T) to orthorhombic (O)– space group $Cmma$) and to the onset of a long range commensurate SDW antiferromagnetic order, respectively.¹³ The latter has been also observed by neutron diffraction measurement as well as by local probe techniques such as muon spin relaxation spectroscopy, ^{57}Fe Mössbauer spectroscopy and ^{139}La and ^{75}As nuclear magnetic resonance (NMR), which all demonstrated the existence of commensurate ordering of the Fe^{2+} ions with a strongly reduced ordered magnetic moment of 0.25-0.36 μ_B .^{14, 15} Theoretical calculations by Yildirim showed that in LaFeAsO the Fe^{2+} ions arranged on a simple square lattice have large next nearest neighbor antiferromagnetic (AF) superexchange interactions mediated by the As ions that give rise to a magnetically frustrated ground state.¹⁶ The structural phase transition (T \rightarrow O) could be driven by a band Jahn-Teller effect that removes the degeneracy of the $\text{Fe}^{2+} 3d_{xz}$ and $3d_{yz}$ orbitals and the magnetic frustration. The lower symmetry of the orthorhombic phase also has effects on the density of states at the Fermi level $N(E_F)$ and on the magnetization providing explanation for the observed drop in the resistivity below 156 K. In the superconducting electron doped systems $\text{LaFeAsO}_{1-x}\text{F}_x$ both the structural phase transition and the SDW instability are suppressed. The relation between magnetic fluctuations and superconductivity has been addressed experimentally by ^{19}F [17] as well as by ^{75}As and ^{139}La NMR [18, 19]. Upon F^- doping, the AF fluctuations disappear and like in high- T_C cuprates a pseudo-gap behavior has been found in the temperature dependence of the ^{19}F [17] and the ^{75}As [18] spin-lattice relaxation rate, T_1^{-1} . In addition, the anisotropy in T_1^{-1} below T_C has been taken as evidence for both a non s -wave type superconductivity and for the existence of line nodes in the superconducting energy gap. It has therefore been pointed out that electron-phonon coupling is probably insufficient to explain the high-temperature superconductivity and that antiferromagnetic interactions or Hund's rule coupling within the multiorbital system should be considered as possible pairing mechanisms.

It is clear that the interplay between magnetism and superconductivity could be responsible for the observed intriguing properties. Within this context, it is important to establish whether similar behavior is encountered in different members of the family. Substitution of La^{3+} with other rare-earth elements such as Nd^{3+} ($4f^7$, $S=3/2$ and effective magnetic moment $\mu_{\text{eff}}=3.6 \mu_B$) introduces

additional spin degrees of freedom in the insulating layer due to the unpaired $4f$ electrons. Interestingly, the $\text{NdFeAs}(\text{O}_{1-x}\text{F}_x)$ family displays superconductivity with enhanced T_c 's of ~ 50 K compared to the La based materials ($T_c \sim 26$ K).^{2, 8} Here we report our studies of the structural and magnetic properties of the parent compound NdFeAsO by means of neutron and X-ray powder diffraction, magnetic susceptibility, ^{75}As NMR and resistivity measurements. In striking contrast with LaFeAsO no commensurate magnetic ordering of the Fe^{2+} sublattice was found between room temperature and 1.6 K, and the wipeout effect of the ^{75}As NMR suggests a highly disordered glass-like state at low temperatures. In addition, the ^{75}As NMR measurements on superconducting $\text{NdFeAsO}_{0.85}\text{F}_{0.15}$ ($T_C = 43$ K) show a completely different behavior from that reported for $\text{LaFeAsO}_{1-x}\text{F}_x$. We found no evidence for pseudo-gap behavior in the spin-lattice relaxation rate T_1^{-1} and ^{75}As NMR shift and the local spin susceptibility is also strongly enhanced.

Results:

The high-resolution neutron and synchrotron X-ray powder diffraction profiles of NdFeAsO at room temperature confirmed that its structure is tetragonal (T) in analogy with other REFeAsO systems. Combined Rietveld analysis of the diffraction patterns, (Fig. 1a,b) resulted in lattice parameters, $a = 3.96342(4)$ Å and $c = 8.5922(1)$ Å with Fe-As and Fe-Fe distances of $2.4007(4)$ Å and $2.80459(1)$ Å, respectively and an As-Fe-As bond angle of $111.39(4)^\circ$. Compared to LaFeAsO , the Nd^{3+} containing oxypnictide shows a contraction of the lattice constants with shorter RE-As bond distances, an increased thickness of the As-Fe₂-As layer and less distorted Fe-As₄ tetrahedra (Table 1).^{13, 20} Temperature dependent synchrotron X-ray powder diffraction measurements collected between room temperature and 100 K revealed the presence of a structural phase transition to an orthorhombic (O) superstructure ($a_O \approx b_O = \sqrt{2}a_T$ and $c_O = c_T$; space group $Cmma$) in analogy with the results reported by Bianconi et al.²¹ All the Bragg reflections containing the tetragonal Miller indexes $h \neq 0$ and $k \neq 0$ start broadening at 160 K (Fig. 1a) and finally split only at 140 K showing that the transition occurs over a broad temperature range. The O phase is robust upon further cooling and Rietveld refinement of the neutron powder diffraction profile at 1.6 K resulted in lattice constants $a = 5.5820(1)$ Å, $b = 5.6119(1)$ Å and $c = 8.5537(1)$ Å with Fe-As and Fe-Fe distances of $2.397(2)$ Å and $2.79102(7)$ Å, respectively. No unusual changes in bond distances and angles are observed between RT and 1.6 K. However, the purely nuclear structural model used in the refinement could not account for two extra peaks which are clearly visible at $Q = 1.12$ and 1.34 Å⁻¹ in the 1.6 K neutron diffraction profile (Fig. 1c). These reflections could be indexed with a magnetic cell directly related to the nuclear structure ($a_M = a_N$, $b_M = b_N$ and $c_M = c_N$) and their intensities could be fitted by considering AF ordering of the Nd^{3+} spins. Neutron diffraction profiles collected at 5 and 50 K do not show the presence of these reflections clearly demonstrating their magnetic origin and a very low ordering temperature T_N (Fig. 1b). Final Rietveld refinement of the 1.6 K neutron diffraction profile shows that in NdFeAsO the magnetic structure is characterized by AF alignment of nearest neighbors Nd^{3+} spins (Fig. 1d) with a magnetic moment of $1.4(1)$ μ_B which is smaller than the calculated value of $\mu_{\text{eff}} = 3.6$ μ_B , perhaps reflecting the close proximity of T_N . These results contrast strongly with the behaviour of LaFeAsO below 130 K, where extra magnetic reflections appear at $Q = 1.15$ and 1.53 and 2.5 Å⁻¹ and could be accounted for by considering long range AF ordering of the Fe^{2+} spins.¹⁴

Resistivity and magnetic susceptibility measurements as a function of temperature and magnetic field also display interesting features (Fig. 2). Between 360 and 250 K, the resistivity decreases slowly with decreasing temperature reaching a shallow minimum at ~ 250 K. Below 250 K, the resistivity starts to increase with decreasing temperature reaching a maximum at 160 K (T_{max}) which also coincides with the temperature where the structural phase transition starts appearing in the diffraction experiments. Below T_{max} the resistivity decreases rapidly to 2 K but no superconducting transition is observed. The plot of $d\rho/dT$ (Fig. 2a) clearly shows a maximum at 140 K that coincides with the temperature where the structural phase transition is completed.

Increasing the magnetic field has little effect on T_{\max} . However, at lower temperatures, large positive magnetoresistances are observed with a maximum value of 60% at 5 K in an applied magnetic field of 9 T. The temperature and field dependences of the resistivity are very similar to those observed for LaFeAsO.^{22, 23} The magnetic properties are, however, very different. The zero field cooled magnetic molar susceptibility (χ_M) of NdFeAsO was measured in applied fields of 10 Oe, 100 Oe and 10 kOe as shown in Fig. 2b. Plots of $\chi_M T$ of the low field data show small anomalies at 160 K and 140 K that then disappear at higher applied magnetic fields. In addition a broad peak centered at 65 K is evident in the 10 Oe data that is again suppressed at higher magnetic fields. Below 50 K, χ_M shows a substantial Curie-Weiss like increase which is attributed to an intrinsic contribution of the Nd³⁺ moments. In agreement with the neutron diffraction findings these results show the absence of long range AFM ordering within the FeAs layer in the O phase. They suggest extreme fragility of the magnetic ground state of FeAs layer where even a small external perturbation, i.e. magnetic fields, can lead to a different magnetic response. As an explanation for the observed behavior, we suggest that the FeAs magnetic state in the O phase is highly disordered characterized by domains with short correlation length. The way these domains interact and percolate depends on the external magnetic field and thus influences the resistivity.

Very interesting features are also observed in the ⁷⁵As NMR temperature dependent spectra of NdFeAsO. We stress that ⁷⁵As NMR is an extremely powerful local probe, which can detect both local structural deformations through the quadrupole interaction $H_Q = \frac{h\nu_Q}{6} \left((3\hat{I}_z^2 - I^2) + \eta(\hat{I}_x^2 - \hat{I}_y^2) \right)$ as well as the local spin susceptibility $\chi(\mathbf{q}=0)$ of the Fe *d* electrons and Nd *f* electrons via the hyperfine coupling interaction. Here $\nu_Q = \frac{3e^2qQ}{2I(2I-1)}$ and $\eta = \frac{V_{xx}-V_{yy}}{V_{zz}}$ are a quadrupole frequency and an asymmetry parameter respectively. The temperature dependence of $\chi(\mathbf{q}=0)$ is deduced from the spin contribution $K_S = A\chi(\mathbf{q}=0)$ to the ⁷⁵As Knight shift $K = K_{orb} + K_S$, where K_{orb} is the powder averaged orbital contribution and A is the hyperfine coupling constant. The ⁷⁵As nuclei lie just above the FeAs plane and have four nearest neighbours Fe atoms (inset to Fig. 3) and reside in the 2c (1/4, 1/4, *z*) position which is axially symmetric. Representative ⁷⁵As NMR spectra measured on powdered NdFeAsO are shown in Fig. 3. The ⁷⁵As NMR spectra display a typical quadrupole powder spectrum for $I = 3/2$ nuclei. At room temperature the shape of the central $-1/2 \leftrightarrow 1/2$ transition and the sharp singularities for the satellite transitions (inset to Fig. 4) strongly indicate an asymmetry parameter $\eta \sim 0$ as is dictated by the tetragonal structure. The ⁷⁵As powder NMR lineshape simulation with $\eta = 0$ (inset to Fig. 4) gives a quadrupole frequency $\nu_Q = 11.8(1)$ MHz. We note that ν_Q is slightly enhanced compared to $\nu_Q = 11.00(5)$ MHz determined for a LaFeAsO_{0.9}F_{0.1} sample [18]. We also stress at this point that a large Knight shift $K = \Delta\nu/\nu_L = 0.42\%$ ($\Delta\nu = \gamma KH_0$ and $\nu_L = \gamma H_0$ is the Larmor frequency) already had to be added to the lineshape simulation at room temperature. With decreasing temperature, the ⁷⁵As resonance rapidly shifts to higher frequencies (Fig. 3). In agreement with the diffraction and resistivity measurements anomalies are observed near T_{\max} (~ 160 K), when the asymmetry parameter η suddenly starts to increase and reaches $\eta = 0.19(2)$ at $T = 132$ K (inset to Fig. S1). This is a clear indication that the T \rightarrow O structural phase transition starts occurring at 160 K but it is complete only at 140 K. Surprisingly, the quadrupole frequency and the line-shift are not affected by the initial onset of the structural phase transition, i.e. ν_Q is temperature independent while the ⁷⁵As Knight shift K monotonically increases with decreasing temperature (Fig. 4). Below ~ 140 K, the ⁷⁵As NMR signal in the parent NdFeAsO starts to rapidly wipe out (Fig. S1) and at 130 K the signal is completely lost (Fig. 3). We note at this point, however, that ¹³⁹La NMR spectra show a typical SDW broadening below $T_{SDW} = 142$ K in LaFeAsO. In NdFeAsO, the ⁷⁵As resonance completely vanishes due to the large spatial modulation of the ⁷⁵As NMR frequency either due to the local magnetic field or to the charge density distribution. The *wipeout* effect in ⁷⁵As NMR strongly suggests the presence of a highly disordered

(glassy) state below 140 K in agreement with the absence of a magnetically ordered phase from neutron diffraction (Fig. 1b) and magnetization measurements (Fig. 2b).

The room temperature synchrotron X-ray diffraction profile of the of the F- doped compound with nominal composition $\text{NdFeAsO}_{0.85}\text{F}_{0.15}$ shows that it adopts a tetragonal structure (space group $P4/nmm$) with reduced lattice constants as compared to the parent compound ($a = 3.96251(1)$ Å and $c = 8.57785(6)$ Å) with Fe-As and Fe-Fe distances of 2.4025(6) Å and 2.80192(1) Å, respectively and an As-Fe-As bond angle of $111.11(4)^\circ$ (Fig. 5). All the distances and bond angles reflect the lattice contraction and no anomalies are observed. We notice that despite the smaller ionic radius of F⁻ as compared to O²⁻, the RE-O distance increases, resulting in an increased thickness of the Nd-O₂-Nd layer and more regular Nd₄-O tetrahedra. No significant changes are observed in the geometry of the As-Fe₂-As layer (Table 1 and Table S2). The temperature dependence of the zero-field cooled magnetization measured under 20 Oe shows the clear onset of bulk superconductivity at $T_C = 43(1)\text{K}$ with shielding fraction of 40 %. The ⁷⁵As NMR spectra measured for $\text{NdFeAsO}_{0.85}\text{F}_{0.15}$ are shown in Fig. 3. Compared to the parent compound the spectra are now considerably broader reflecting the structural disorder and strains introduced by the F-doping, preventing the precise determination of the asymmetry parameter. The quadrupole frequency has, however, significantly increased by nearly 9 %, i.e. $\nu_Q = 12.8(6)$ MHz, compared to the value of undoped NdFeAsO. The lattice contraction in the F-doped sample explains the observed increase in ν_Q . On cooling, the ⁷⁵As NMR spectra gradually shift to higher frequencies with decreasing temperature. In contrast to the parent compound we can easily measure the ⁷⁵As NMR signal even for $T < 130$ K as the magnetic and/or charge fluctuations responsible for the wipeout effect present in undoped NdFeAsO have been suppressed by electron doping. For the temperature range between room temperature and 50 K, the shift of the ⁷⁵As resonance follows a Curie-Weiss like behavior (Fig. 4), i.e. $\Delta\nu(T) = \Delta\nu_0 + \kappa(T - \theta)$ with $\Delta\nu_0 = 66(10)$ kHz, $\kappa = 63(5)$ MHz.K, and $\theta = -11(1)$ K. We stress here that we found no indication for pseudo-gap like behavior of $\Delta\nu$ as reported in $\text{LaFeAsO}_{1-x}\text{F}_x$ from the ⁷⁵As and ¹⁹F NMR [17, 18]. Below the superconducting transition, the resonance rapidly broadens and we were not able to measure spectra with satisfactory signal to noise ratio below 38 K.

We have also measured the ⁷⁵As spin-lattice relaxation rate T_1^{-1} for both parent and F-doped samples. For NdFeAsO, the $(T_1T)^{-1}$ parameter is nearly temperature independent between room temperature and ~ 170 K (inset to Fig. 6). In the T phase spin-lattice relaxation therefore obeys the Korringa relation. We also note at this point that the $(T_1T)^{-1}$ parameter, at room temperature, is nearly an order of magnitude larger (or T_1 is by an order of magnitude smaller) than has been measured in $\text{LaFeAsO}_{0.9}\text{F}_{0.1}$ [18]. This clearly shows that the dominant relaxation mechanism in the NdFeAsO-based materials is completely different to that encountered in $\text{LaFeAsO}_{1-x}\text{F}_x$ and must involve an additional relaxation channel. Below ~ 160 K $(T_1T)^{-1}$ becomes progressively enhanced with decreasing temperature and shows a weakly divergent behaviour below ~ 140 K. The critical slowing down of spin or charge fluctuations below 160 K is more gradual than that observed in LaFeAsO, undergoing a magnetic (SDW) phase transition. In $\text{NdFeAsO}_{0.85}\text{F}_{0.15}$, $(T_1T)^{-1}$ measured on both singularities (labeled as A and B singularities in Fig. 3) is equivalent to the parent compound at high temperatures (Fig. 6). In the normal state almost no anisotropy is observed in T_1^{-1} . With decreasing temperature $(T_1T)^{-1}$ becomes progressively enhanced and its temperature dependence closely mimics K^2 therefore confirming the Korringa relation within the experimental uncertainty for the F-doped sample. This finding is surprising as it is believed that the Fe *d* electrons are strongly correlated. The proximity of the SDW instability spin fluctuation spectrum due to the magnetic interactions may change and provide an efficient relaxation mechanism. The anisotropy in $(T_1T)^{-1}$ starts to develop below T_C where the high frequency singularity B (i.e. for the crystalline orientation where the angle between the external magnetic field and the *z*-principle axis of the EFG tensor is $\theta = 90^\circ$) has a slightly stronger relaxation rate. However, very surprisingly we did not observe a reduction in $(T_1T)^{-1}$ below T_C in the superconducting state as has been observed in La-

based samples. Unfortunately the rapid disappearance of the ^{75}As NMR signal below T_C prevented us to measure T_1^{-1} well below 35 K where the opening of the superconducting gap is expected to reduce T_1^{-1} . It may well be, that the observed behaviour of $(T_1T)^{-1}$ below T_C reflects a Hebel-Slichter coherence peak not observed for $\text{LaFeAsO}_{0.9}\text{F}_{0.1}$ sample.¹⁸

Discussion:

The diffraction profile of NdFeAsO at 1.6 K does not show any magnetic peaks originating from the long range ordering of the Fe^{2+} sublattice. Instead, AF ordering of the Nd^{3+} moments is observed at 1.6 K. The magnetic susceptibility reveals a broad hump below 65 K in low magnetic fields, suggesting the presence of short range AF correlations and the absence of any kind of commensurate magnetic ordering of the Fe^{2+} ions. In addition, the ^{75}As NMR shift and the spin-lattice relaxation rate $(T_1T)^{-1}$ and the *wipeout* effect measured for the parent compound imply a highly disordered state below 140 K with large spin and/or charge spatial inhomogeneities setting in already at around 160 K. These observations are dramatically different from LaFeAsO . Moreover, the ^{75}As NMR shift and the spin-lattice relaxation rate $(T_1T)^{-1}$ measured for F-doped NdFeAsO increase monotonically with decreasing temperature and do not show a pseudo-gap type of behavior like the F⁻ doped LaFeAsO materials. These results point towards a more complex phase diagram of NdFeAsO compared to the La based superconductor. The obvious difference between the two families is the magnetic moment associated with the RE ion: La^{3+} is nonmagnetic while Nd^{3+} has a large magnetic moment bringing an extra degree of freedom into the system. The electronic structure calculated within Density Functional Theory (DFT) for $\text{LaFeAsO}_{1-x}\text{F}_x$ [12] shows a strong hybridization only between the Fe 3*d* and As 4*p* orbitals explaining large shift of the ^{75}As NMR resonance. Mixing of Fe 3*d* and O 2*p* orbitals is predicted to be negligible. If $\text{NdFeAsO}_{1-x}\text{F}_x$ has a similar electronic structure, then this would imply that the local spin susceptibility $\chi(\mathbf{q}=0)$ measured by the ^{75}As NMR shift depends only on the spin response of the conducting FeAs layer and not on the NdO layer. Based on these arguments, the ^{75}As shifts in $\text{LaFeAsO}_{1-x}\text{F}_x$ and $\text{NdFeAsO}_{1-x}\text{F}_x$ should be rather similar. In order to account for the measured anomalous difference and temperature dependence of $\Delta\nu$ (Fig. 4) one may consider the temperature dependence of localized Nd^{3+} moments and couple them to FeAs itinerant electrons. This would require the introduction of higher order effects like small hybridization between the O-*p* and As-*p* orbitals for instance. Alternatively, recent calculations of local susceptibility using LDA+DMFT method [24] showed how sensitive the ground state could be to the size of Hund's rule coupling. Namely, it was demonstrated that the Hund's rule coupling J_{Hund} dramatically reduces the coherence scale in oxypnictides and promotes highly incoherent metallic state. For intermediate values of $J_{Hund} \sim 0.35\text{-}0.4$ eV, the calculated local susceptibility of the iron atom changes from Pauli-like to Curie-like as the temperature decreases. This reflects the transition from an incoherent metal to the coherent Fermi liquid at low temperature. We note that the temperature dependence of the ^{75}As NMR shifts measured here in NdFeAsO and $\text{NdFeAsO}_{0.85}\text{F}_{0.15}$ samples qualitatively agrees with this picture.

In conclusion, neutron and X-ray powder diffraction, magnetic susceptibility, resistivity and ^{75}As nuclear magnetic resonance (NMR) measurements were performed on the parent NdFeAsO and electron doped $\text{NdFeAsO}_{0.85}\text{F}_{0.15}$. In striking contrast to the La based family, no AF long range ordered Fe phase has been found and the ground state has a strong spin and/or charge spatial disorder. In addition, no evidence for the pseudo-gap has been found and the ^{75}As shift as well as $(T_1T)^{-1}$ increase with decreasing temperature in F-doped superconducting $\text{NdFeAsO}_{0.85}\text{F}_{0.15}$. These results show that the RE ions are not innocent spectators and that their magnetic moments introduce extra degrees of freedom into the system strongly influencing the ground state properties and adding complexity to the electronic and magnetic phase diagrams. It is very appealing at this point to draw an analogy between NdFeAsO and cuprates where a very complex phase diagram has been developed in the small doping regime including AF, stripe and spin-glass (SG) phases.²⁵ It may well be, that in NdFeAsO , due to the Nd^{3+} moment a SG or stripe phase^{26, 27} may develop below ~

140 K. This scenario is very different from the one developed for the La based oxypnictides where, upon doping, the AF ordered phase develops directly into a pseudogap phase. More experimental and theoretical efforts are needed to identify the key factors leading to the high-temperature superconducting mechanism with particular attention devoted to the low doping region.

Experimental:

Polycrystalline NdFeAsO and NdFeAsO_{0.85}F_{0.15} samples were prepared by a two-step solid state reaction method. Stoichiometric amounts of NdAs (prepared by reacting Nd and As at 900 °C for 12 hours), Fe, Fe₂O₃ and NdF₃ were homogenized using mortar and pestle and pressed into pellets using an 8 mm steel die and 10 tonne press. The pellets were inserted in tantalum cells and then heated in vacuum sealed quartz tubes for 2 x 24 hours at 1150 °C with an intermediate homogenization. The magnetic susceptibilities were measured using a Quantum Design Magnetic Property Measurement System. The samples were zero field cooled and measured on heating in at different applied magnetic fields. The electrical resistivity of NdFeAsO was measured on a rectangular bar using a Quantum Design Physical Property Measurement System. The temperature dependences were collected on heating from 2 K to 350 K on a ramp of 1K/min. Neutron powder diffraction data on NdFeAsO were collected on the D2B high-resolution powder diffractometer at the ILL in Grenoble, France. Datasets were recorded between $5 \leq 2\theta \leq 160^\circ$ with a step-size of 0.05° at temperatures of 1.6 K, 5K, 50K, 175 K and RT. The neutron wavelengths used were 1.594 Å and 2.40 Å. Synchrotron powder diffraction data on parent and doped samples were collected on the ID31 high-resolution diffractometer at the European Synchrotron Radiation Facility in Grenoble, France. Datasets were recorded on cooling (1 K/min) between 175 and 100 K, and were binned with a 0.002° stepsize ($\lambda=0.3999$ Å). The GSAS suite of programs and EXPGUI graphical user interface were used for Rietveld fitting [28, 29]. ⁷⁵As NMR (spin $I = 3/2$) experiments were performed at a magnetic field of 8.9 T. The corresponding reference frequency of $\nu(^{75}\text{As}) = 65.096$ MHz was determined from a NaAsF₆ standard. Frequency-swept spectra were measured with a selective solid echo pulse sequence ($\pi/2$) - τ - ($\pi/2$) - τ - (echo), with a pulse length $\pi/2 = 22$ μs and interpulse delay $\tau = 50$ μs . Repetition time was 0.1 s at ambient temperature. For ⁷⁵As spin-lattice relaxation measurements the inversion recovery technique was applied.

Figure captions:

Figure 1. Final observed (O) and calculated (-) synchrotron X-ray (a) [$\lambda=0.39985$ Å, RT] and neutron powder diffraction (b, c) ($\lambda=1.594$ Å, RT and 1.6 K) profiles for NdFeAsO. The lower solid lines show the difference profiles and the tick marks show the reflection positions [in (a, b): top: NdFeAsO, bottom: NdAs, in (c): top NdFeAsO, bottom: magnetic phase]. The insets illustrate the T-O structural phase transition at 140 K, the magnetic Bragg reflections at 1.6 K, and the disappearance of the magnetic reflections at 5 K. The magnetic structure is illustrated in Fig. 1(d).

Figure 2. Temperature and field evolution of the resistivity (a) and zero field cooled magnetic susceptibility (b). The insets illustrate the 9 Tesla magnetoresistance in the vicinity of the structural phase transition and T_{max} , the large positive magnetoresistances at low temperature and the high temperature magnetic susceptibility via $(M/H)*T$.

Figure 3. Representative ^{75}As NMR spectra measured in parent undoped NdFeAsO (a) and F-doped NdFeAsO_{0.85}F_{0.15} powder sample (b). Inset: Structure around the As ion showing its distances to nearest neighboring Fe ions (black spheres) and Nd ions (white spheres) in the neighboring NdO layer.

Figure 4. Temperature dependence of the ^{75}As NMR shift measured for undoped NdFeAsO (open circles) and F-doped NdFeAsO_{0.85}F_{0.15} powder samples (solid circles). For comparison we show the corresponding shift measured in LaFeAsO_{0.9}F_{0.1} (data adapted from reference [18]). For NdFeAsO and NdFeAsO_{0.85}F_{0.15} the shift has been determined from the ^{75}As NMR lineshape simulations as exemplified for the case of spectrum measured in parent compound at $T = 180$ K (inset).

Figure 5. Final observed (O) and calculated (-) synchrotron X-ray powder diffraction profiles ($\lambda=0.39985$ Å) for NdFeAsO_{0.85}F_{0.15} RT. The lower solid lines show the difference profiles and the tick marks show the reflection positions (from top to bottom: NdFeAsO_{0.85}F_{0.15}, Fe, NdAs and NdOF). The insets illustrates the temperature dependence of the magnetization, M (ZFC, 20 Oe) for NdFeAsO_{0.85}F_{0.15} showing a superconducting transition temperature of 42 K and a shielding fraction of 40.6 %.

Figure 6. Temperature dependence of ^{75}As $(T_1T)^{-1}$ for NdFeAsO (solid circles) and NdFeAsO_{0.85}F_{0.15} measured on low-frequency singularity (A, solid triangles) and high-frequency singularity (B, open triangles). Inset: ^{75}As $(T_1T)^{-1}$ is shown for NdFeAsO only.

Figure S1. Temperature dependence of ^{75}As normalized intensity for NdFeAsO (solid circles) and NdFeAsO_{0.85}F_{0.15} measured on low-frequency singularity (A, solid triangles) and high-frequency singularity (B, open triangles). Inset: Temperature dependence of ^{75}As asymmetry parameter η for NdFeAsO only.

Table 1. Comparison of lattice constants, selected bond lengths and angles, and layer thickness between LaFeAs(O,F) and NdFeAs(O,F). The data for LaFeAs(O,F) are taken from [13].

	LaFeAsO	LaFeAsO _{0.86} F _{0.14}	NdFeAsO	NdFeAsO _{0.85} F _{0.15}
<i>a</i> -axis (Å)	4.03268(1)	4.02460(2)	3.96629(1)	3.96251(1)
<i>c</i> -axis (Å)	8.74111(4)	8.69525(5)	8.59886(6)	8.57785(6)
RE-As (4x)	3.3773	3.3331	3.3070(4)	3.2830(5)
RE-O (4x)	2.3647	2.3851	2.3149(3)	2.3262(3)
Fe-As (4x)	2.4131	2.4132	2.4007(4)	2.4025(6)
As-Fe-As (2x)	113.35	113.00	111.39(3)	111.11(4)
As-Fe-As (4x)	107.57	107.74	108.52(2)	108.66(2)
RE-O-RE (2x)	117.01	115.07	117.89(2)	116.79(2)
RE-O-RE (4x)	105.84	106.75	105.43(1)	105.94(1)
As-Fe ₂ -As // <i>c</i> -axis	2.6514(6)	2.6641(9)	2.7061(8)	2.7175(9)
RE-O ₂ -RE // <i>c</i> -axis	2.4709(3)	2.5606(5)	2.3883(5)	2.4380(5)
RE-As // <i>c</i> -axis	1.8094(7)	1.735(1)	1.7523(9)	1.711(1)

Figure 1.

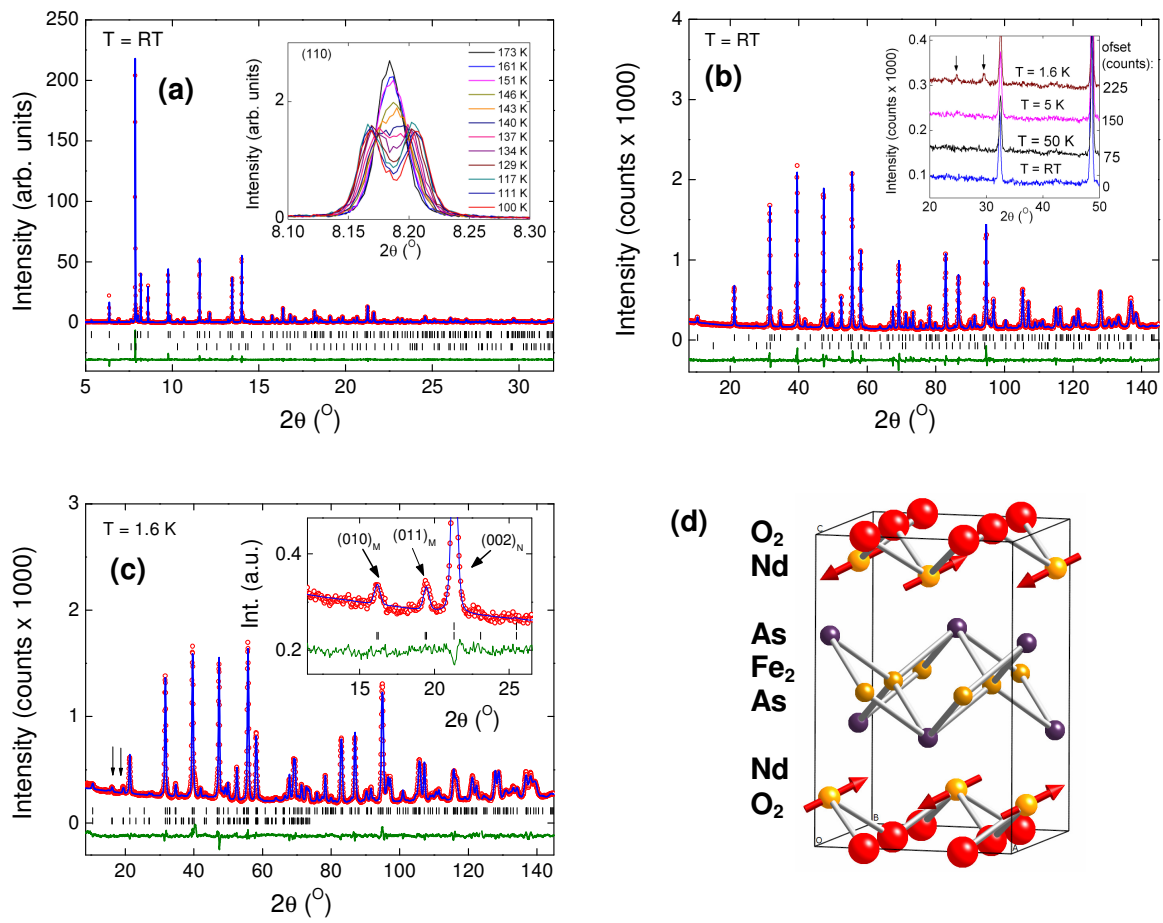


Figure 2.

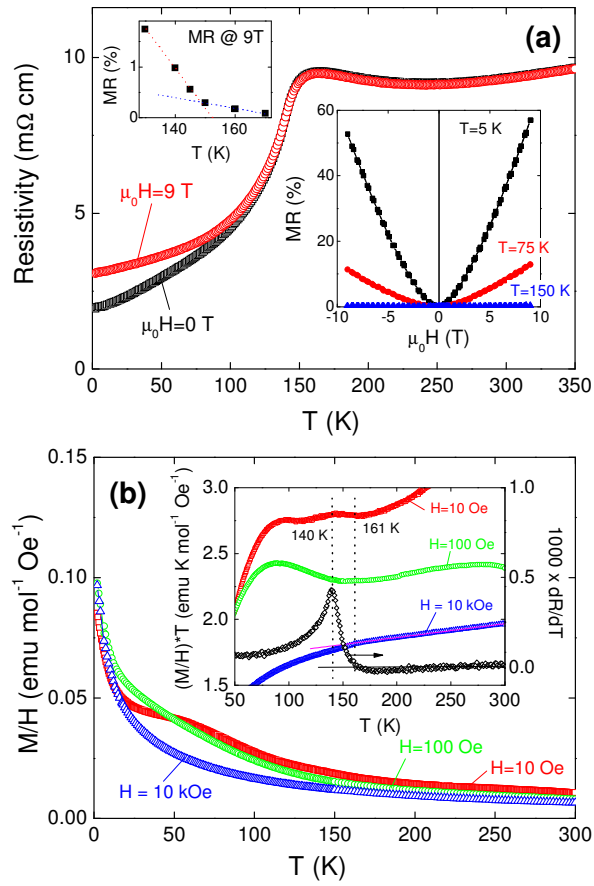


Figure 3.

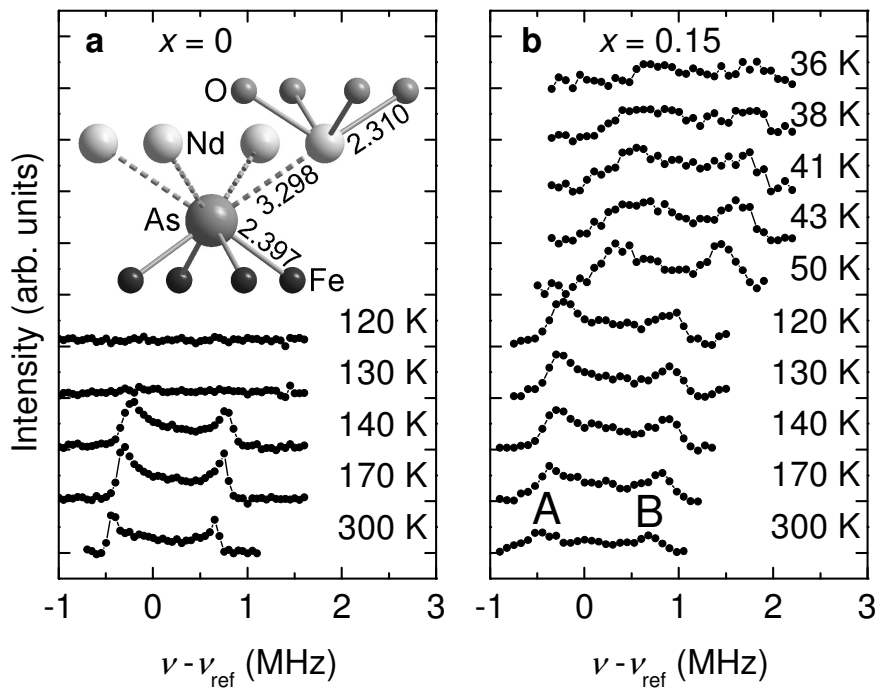


Figure 4.

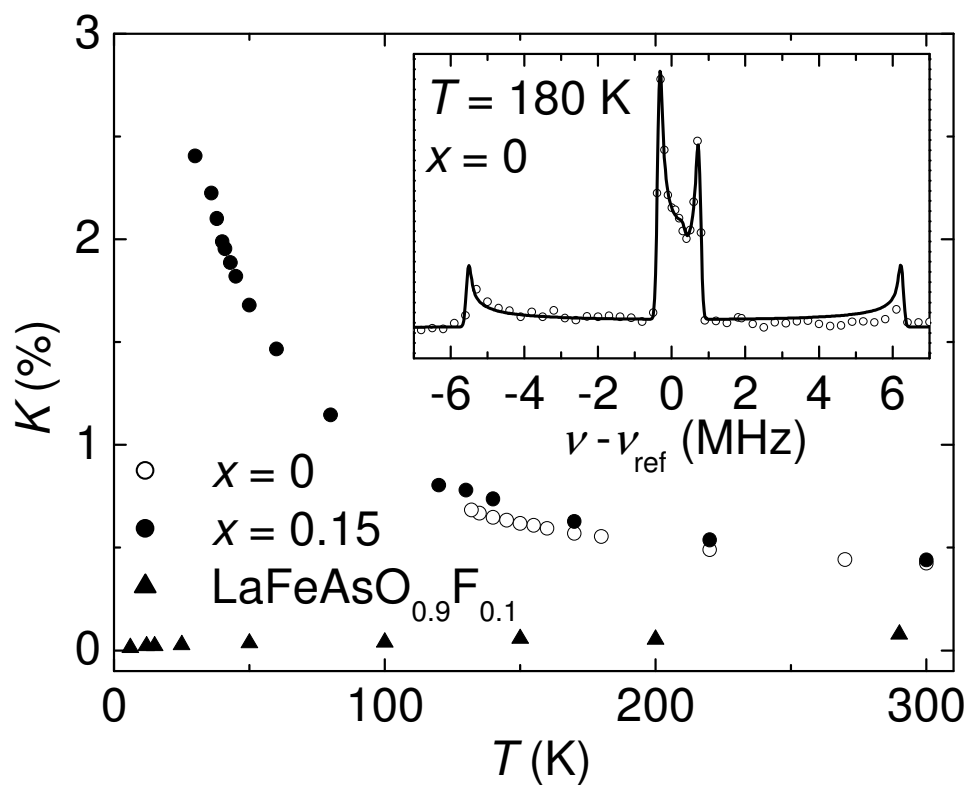


Figure 3.

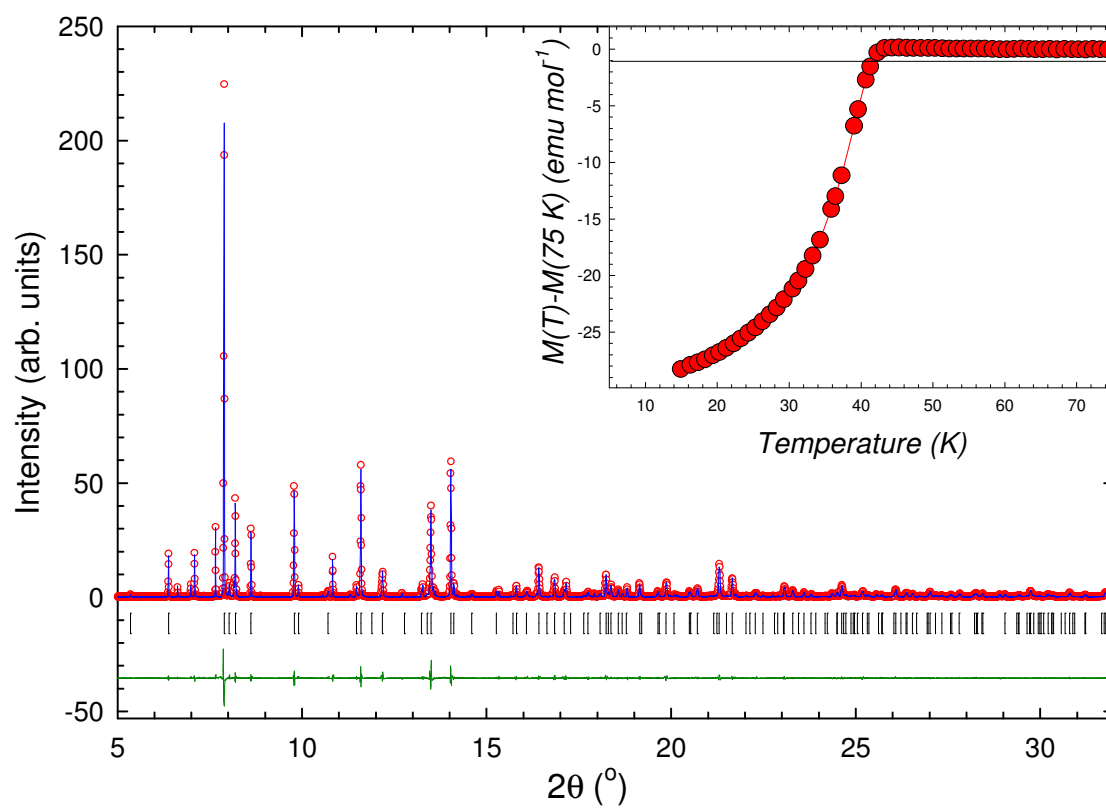


Figure 6.

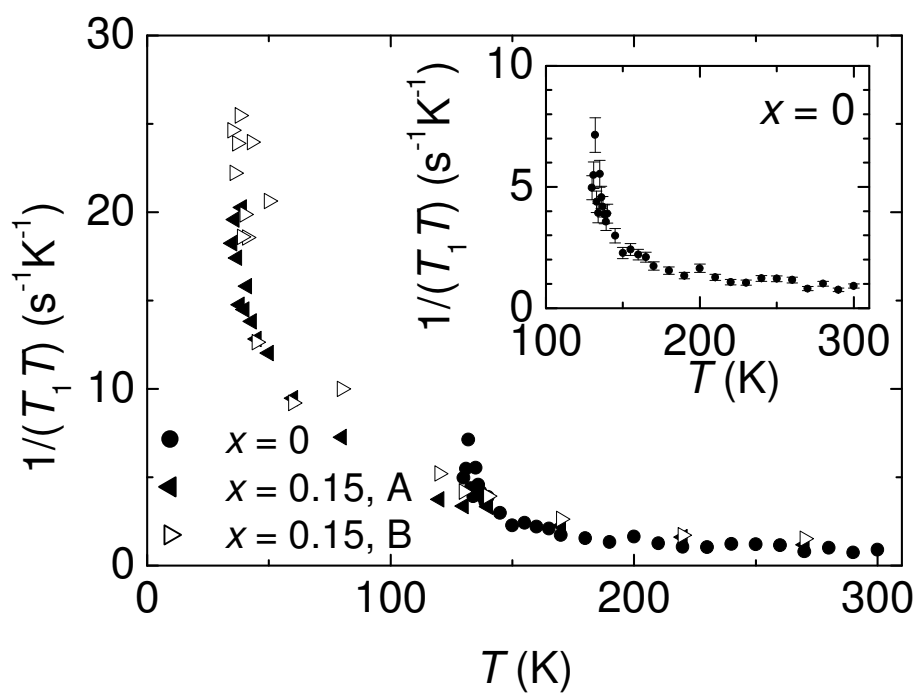


Table S1. Refined lattice constants, atomic parameters and selected bond lengths (Å) and angles (°) for at room temperature (RT), 175 K and 1.6 K from synchrotron X-ray and neutron powder diffraction measurements.

		RT	175 K	1.6 K
SG		<i>P4/nmm</i>	<i>P4/nmm</i>	<i>Cmma</i>
<i>a</i> -axis (Å)		3.96629(1)	3.95890(6)	5.5820(1)
<i>b</i> -axis (Å)				5.6119(1)
<i>c</i> -axis (Å)		8.59886(6)	8.5720(2)	8.5537(3)
Volume (Å ³)		135.272(1)	134.348(6)	267.95(1)
Nd	<i>z</i>	0.13887(6)	0.1390(3)	0.1390(3)
	U _{iso}	0.0065(6)	0.0034(6)	0.0010(6)
	Occ.	1.02(1)	1.00	1.00
O	U _{iso}	0.0080(8)	0.0072(8)	0.0062(8)
	Occ.	1.00(1)	1.00	1.00
Fe	U _{iso}	0.0071(5)	0.0074(6)	0.0057(6)
	Occ.	1.00	1.00	1.00
As	<i>z</i>	0.65735(9)	0.6576(3)	0.6581(3)
	U _{iso}	0.0080(8)	0.0082(7)	0.0064(7)
	Occ.	0.99(1)	1.00	1.00
χ^2		2.4	2.6	2.5
wRp (%)		13.2 (xrd) 4.5 (nd)	5.3	5.3
Rp (%)		9.2 (xrd) 3.5 (nd)	4.1	4.2
R _F ² (%)		4.3 (xrd) 4.0 (nd)	3.8	4.8
Nd-As		3.3070(4) (4x)	3.298(1) (4x)	3.300(1) (2x) 3.287(1) (2x)
Nd-O		2.3149(3) (4x)	2.310(1) (4x)	2.309(1) (4x)
Fe-As		2.4007(4) (4x)	2.397(2) (4x)	2.397(2) (4x)
Fe-Fe		2.80459(1) (4x)	2.79937(4) (4x)	2.79102(7) (2x) 2.80597(7) (2x)
Fe-As-Fe		111.39(3) 71.48(2) (4x)	111.4(1) (2x) 71.47(6) (4x)	111.3(1) (2x) 71.22(6) (2x) 71.66(6) (2x)
Nd-O-Nd		117.89(2) (2x) 105.43(1) (4x)	117.90(9) (2x) 105.42(4) (4x)	118.01(9) (2x) 105.61(4) (2x) 105.15(4) (2x)

P4/nmm: Nd on 2*c* (1/4, 1/4, *z*), Fe on 2*b* (3/4, 1/4, 1/2), O on 2*a* (3/4, 1/4, 0), As on 2*c* (1/4, 1/4, *z*).

Cmma: Nd on 4*g* (0, 1/4, *z*), Fe on 4*b* (1/4, 0, 1/2), O on 4*a* (1/4, 0, 0), As on 4*g* (0, 1/4, *z*).

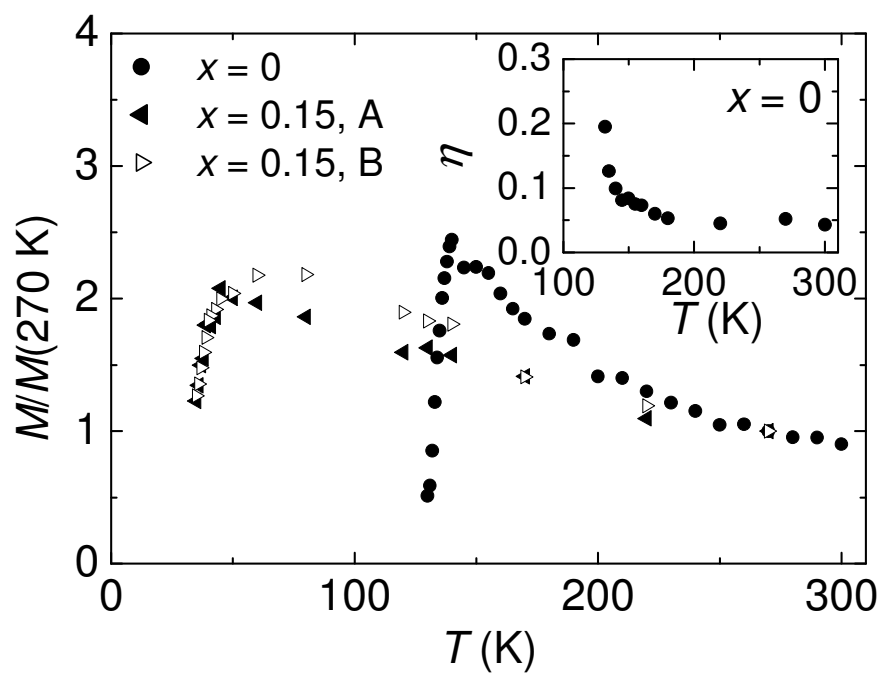
Weight fractions: NdFeAsO: 0.95, NdAs: 0.05.

Table S2. Refined lattice constants, atomic parameters and selected bond lengths (Å) and angles (°) for NdFeAsO_{0.87(3)}F_{0.13(3)} at room temperature from synchrotron X-ray powder diffraction measurements.

SG		RT
		<i>P4/nmm</i>
<i>a</i> -axis (Å)		3.96251(1)
<i>c</i> -axis (Å)		8.57785(6)
Volume (Å ³)		134.685(1)
Nd	<i>z</i>	0.14211(6)
	U _{iso}	0.0075(1)
	Occ.	0.98(1)
O	U _{iso}	0.014(3)
	Occ.	0.87(3)
F	U _{iso}	0.014(3)
	Occ.	0.13(3)
Fe	U _{iso}	0.0072(4)
	Occ.	1.00(2)
As	<i>z</i>	0.6544(1)
	U _{iso}	0.0059(3)
	Occ.	0.99(2)
χ^2		2.4
wRp (%)		12.84
Rp (%)		10.31
R _F ² (%)		3.89
Nd-As		3.2830(5) (4x)
Nd-O		2.3262(3) (4x)
Fe-As		2.4025(6) (4x)
Fe-Fe		2.80192(1) (4x)
Fe-As-Fe		111.11(4)
		71.24(2) (2x)
Nd-O-Nd		116.79(2) (2x)
		105.94(1) (4x)

P4/nmm: Nd on 2*c* (1/4, 1/4, *z*), Fe on 2*b* (3/4, 1/4, 1/2), O on 2*a* (3/4, 1/4, 0), As on 2*c* (1/4, 1/4, *z*).
Weight fractions: Fe: 2.2(1) % NdAs: 5.2(2)% , NdOF: 6.8(4)%.

Figure S1.



References

1. Quebe, P., Terbuchte, L. J. & Jeitschko, W. Quaternary rare earth transition metal arsenide oxides RTAsO (T=Fe, Ru, Co) with ZrCuSiAs type structure J. Alloys Compounds 302, 70 (2000).
2. Kamihara, Y., Watanabe, T., Hirano, M. & Hosono, H. Iron-based layered superconductor La[O_{1-x}F_x]FeAs (x=0.05-0.12) with T_c=26 K J. Am. Chem. Soc., 3296 (2008).
3. Takahashi, H. et al. Superconductivity at 43 K in an iron-based layered compound LaO_{1-x}F_xFeAs. Nature 453, 376-378 (2008).
4. Wen, H. H., Mu, G., Fang, L., Yang, H. & Zhu, X. Y. Superconductivity at 25K in hole-doped (La_{1-x}Sr_x) OFeAs. EPL 82, 17009 (2008).
5. Ren, Z.-A. et al. Superconductivity and Phase Diagram in the Iron-based Arsenic-oxides ReFeAsO_{1-δ} (Re = rare earth metal) without F-Doping. arXiv:0804.2582 (2008).
6. Chen, G. F. et al. Superconductivity at 41 K and its competition with spin-density-wave instability in layered CeO_{1-x}F_xFeAs. arXiv:0803.3790v3 (2008).
7. Ren, Z.-A. et al. Superconductivity at 52 K in iron-based F-doped layered quaternary compound Pr[O_{1-x}F_x]FeAs. arXiv:0803.4283 (2008).
8. Ren, Z.-A. et al. Superconductivity in iron-based F-doped layered quaternary compound Nd[O_{1-x}F_x]FeAs. arXiv: 0803.4234 (2008).
9. Chen, X. H. et al. Superconductivity at 43 K in SmFeAsO(1-x)F(x). Nature, doi:10.1038/nature07045 (2008).
10. Cheng, P. et al. Superconductivity at 36 K in gadolinium-arsenide oxides GdO_{1-x}F_xFeAs. Science in China Series G-Physics Mechanics & Astronomy 51, 719-722 (2008).
11. Bos, J. W. G. et al. High pressure synthesis of late rare earth RFeAs(O,F) superconductors; R = Tb and Dy. arXiv:0806.0926 (2008).
12. Haule, K., Shim, J. H. & Kotliar, G. Correlated electronic structure of LaOFeAs. Physical Review Letters 100, 226402 (2008).
13. Nomura, T. et al. Crystallographic Phase Transition and High-T_c Superconductivity in LaOFeAs:F. arXiv:0804.3569v1 (2008).
14. Cruz, C. d. I. et al. Magnetic Order versus superconductivity in the Iron-based layered La(O_{1-x}F_x)FeAs systems. doi:10.1038/nature07057 (2008).
15. Klauss, H.-H. et al. Commensurate Spin Density Wave in LaOFeAs: A Local Probe Study. arXiv:0805.0264 (2008).
16. Yildirim, T. Origin of the ~150 K Anomaly in LaOFeAs; Competing Antiferromagnetic Superexchange Interactions, Frustration, and Structural Phase Transition. arXiv:0804.2252v1 (2008).
17. Ahilan, K. et al. 19-F NMR Investigation of LaAsFeO(0.89)F(0.11) Superconductor. arXiv:0804.4026 (2008).
18. Grafe, H.-J. et al. 75As NMR studies of superconducting LaO_{0.9}F_{0.1}FeAs. arXiv:0805.2595 (2008).
19. Nakai, Y., Ishida, K., Kamihara, Y., Hirano, M. & Hosono, H. Evolution from Itinerant Antiferromagnet to Unconventional Superconductor with Fluorine Doping in La(O_{1-x}F_x)FeAs Revealed by ⁷⁵As and ¹³⁹La Nuclear Magnetic Resonance. arXiv:0804.4765 (2008).
20. McQueen, T. M. et al. Intrinsic Properties of Stoichiometric LaOFeP. arXiv:0805.2149v1 (2008).
21. Fratini, M. et al. The effect of internal pressure on the tetragonal to monoclinic structural phase transition in ReOFeAs: the case of NdOFeA. arXiv:0805.3992 (2008).
22. Dong, J. et al. Competing Orders and Spin-Density-Wave Instability in La(O_{1-x}F_x)FeAs. arXiv:0803.3426 (2008).
23. Zhu, X., Yang, H., Fang, L., Mu, G. & Wen, H.-H. Upper critical field, Hall effect and magnetoresistance in the iron-based layered superconductor LaO_{0.9}F_{0.1-δ}FeAs. arXiv:0803.1288 (2008).
24. Haule, K. & Kotliar, G. Coherence-incoherence crossover in the normal state of iron-oxypnictides and importance of the Hund's rule coupling. arXiv:0805.0722 (2008).
25. Dagotto, E. Complexity in strongly correlated electronic systems. Science 309, 257-262 (2005).
26. Hunt, A. W., Singer, P. M., Thurber, K. R. & Imai, T. Cu-63 NQR measurement of stripe order parameter in La_{2-x}Sr_xCuO₄. Physical Review Letters 82, 4300-4303 (1999).
27. Tranquada, J. M., Sternlieb, B. J., Axe, J. D., Nakamura, Y. & Uchida, S. Evidence for Stripe Correlations of Spins and Holes in Copper-Oxide Superconductors. Nature 375, 561-563 (1995).

28. Larson, A. C. & Von Dreele, R. B. Los Alamos National Laboratory Report LAUR, 86 (2000).
29. Toby, B. H. EXPGUI. Journal of Applied Crystallography 34, 210 (2001).